Bulg. J. Phys. **44** (2017) S93–S104

Bounds on the Speed of Sound, Tidal Polarizability and Gravitational Waves from Neutron Stars

Ch.C. Moustakidis, **T. Gaitanos**, **Ch. Margaritis**, **G.A. Lalazissis**
Department of Theoretical Physics, Aristotle University of Thessaloniki, 54124 Thessaloniki, Greece

Received *23 June 2017*

Abstract. The accurate determination of the maximum mass of the neutron stars is one of the most important tasks in astrophysics. It is directly related to the identification of the black holes in the universe, the production of neutron stars from the supernovae explosion, and the equation of state (EoS) of dense matter. The speed of sound in dense matter is also a crucial quantity which characterizes the stiffness of the EoS since its upper bound imposes strong constraints on the maximum mass of neutron stars. However, this upper bound remains still an open issue. In the present work we study possible effects of the upper bound of the speed of sound on the upper bound of the mass and the tidal polarizability. We conclude that these kinds of measurements, combined with recent observations of neutron stars with masses close to $2M_{\odot}$, will provide robust constraints on the equation of state of hadronic matter at high densities.

PACS codes: 26.60.-c, 21.30.Fe, 21.65.Cd, 26.60.Kp

1 Introduction

The determination of the maximum mass of a neutron star (NS) (rotating and nonrotating) is one of the long-standing subjects in astrophysics (for a comprehensive introduction dedicated to this problem see Ref. [1]). In particular, the identification of a black hole requires the knowledge of the maximum mass of a neutron star. The maximum neutron star mass is of considerable interest in the study of the production of neutron stars and black holes in the dynamics of supernovae explosion. Moreover, the experimental observations of neutron star masses have imposed strong constraints on the hadronic equation of state (EoS) of superdense matter (see also the references about the neutron star mass distribution [2, 3]). The most famous examples are the recent discoveries of massive neutron stars with gravitational masses of $M = 1.97 \pm 0.04\ M_{\odot}$ (PRS J1614-2230 [4]) and $M = 2.01 \pm 0.04\ M_{\odot}$ (PSR J0348+0432 [5]).

From a theoretical point of view, it is well known that the exact value of the maximum mass $M_{\max}$ of an NS depends strongly on the EoS of β-stable nuclear matter [6]. Despite intensive investigations, the upper bound of neutron stars remains up to present uncertain [7–11]. One possibility of proceeding with an estimate of $M_{\max}$ is based on the pioneering idea of Rhoades and Ruffini [7], where an optimum upper bound of mass of non-rotating neutron stars was derived using a variational technique. An issue was raised recently concerning the high-density upper bound of the speed of sound. The speed of sound v_s, because of the causality, should not exceed that of light. Recently, Bedaque and Steiner [12] have provided simple arguments that support the limit $c/\sqrt{3}$ in non-relativistic and/or weakly coupled theories. The authors pointed out that the existence of neutron stars with masses about two solar masses combined with the knowledge of the EoS of hadronic matter at low densities is not consistent with this bound. The main motivation of the present paper is to study in detail the limiting cases of the upper bound of the speed of sound and their effects on the bulk neutron star properties. We use a class of equation of states, which have been extensively employed in the literature and mainly have the advantage to predict neutron star masses close or higher to the experimentally observed value of $2M_{\odot}$ [4, 5].

2 Nuclear Equation of State and the Maximum Mass Configuration

It is known that no bounds can be determined for the mass of non-rotating neutron stars without some assumptions concerning the properties of neutron star matter [1]. In this study, following the work of Sabbadini and Hartle [13] we consider the following four assumptions: (i) the matter of the neutron star is a perfect fluid described by a one-parameter equation of state between the pressure P and the energy density $\mathcal{E}$, (ii) the energy density $\mathcal{E}$ is non-negative (because of the attractive character of gravitational forces), (iii) the matter is microscopically stable, which is ensured by the conditions $P \geq 0$ and $dP/d\mathcal{E} \geq 0$ and (iv) below a critical baryon density n_0 the equation of state is well known. Furthermore, we introduce two regions for specifying more precisely the EoS. The radius R_0 at which the pressure is $P_0 = P(n_0)$, divides the neutron star into two regions. The core, where $r \leq R_0$ and $n \geq n_0$ and the envelope where $r \geq R_0$ and $n \leq n_0$. The adiabatic speed of sound is defined as $\dfrac{v_s}{c} = \sqrt{\left(\dfrac{\partial P}{\partial \mathcal{E}}\right)_S}$ where S is the entropy per baryon [14]. In the present work we consider the following two upper bounds for the speed of sound: (a) $\dfrac{v_s}{c} \leq 1$ (causality limit from special relativity (see [1] and reference therein)) and (b) $\dfrac{v_s}{c} \leq \dfrac{1}{\sqrt{3}}$ (from QCD and other theories (see [12] and reference therein)).

We construct the maximum mass configuration by considering the following structure for the neutron star EoS

$$P(\mathcal{E}) = \begin{cases} P_{crust}(\mathcal{E}), & \mathcal{E} \leq \mathcal{E}_{\rm c-edge} \\ P_{NM}(\mathcal{E}), & \mathcal{E}_{\rm c-edge} \leq \mathcal{E} \leq \mathcal{E}_0 \\ \left(\frac{v_S}{c}\right)^2 (\mathcal{E} - \mathcal{E}_0) + P_{NM}(\mathcal{E}_0), & \mathcal{E}_0 \leq \mathcal{E}. \end{cases} \quad (1)$$

According to Eq. (1), the EoS yielding the maximum mass of neutron stars, is divided into three regions. In particular, above the critical energy density $\mathcal{E}_0$ the EoS is maximally stiff with the speed of sound $\sqrt{\left(\frac{\partial P}{\partial \mathcal{E}}\right)_S}$ fixed in the interval $\left(1/\sqrt{3} - 1\right) c$. In the intermediate region $\mathcal{E}_{\rm c-edge} \leq \mathcal{E} \leq \mathcal{E}_0$ we employed a specific EoS which is used for various nuclear models (see below for more details), while for $\mathcal{E} \leq \mathcal{E}_{\rm c-edge}$ we used the EoS given in Ref. [15]. The crust-core interface energy density $\mathcal{E}_{\rm c-edge}$, between the liquid core and the solid crust is determined by employing the thermodynamical method [16].

We use the following notations and specifications for the results of the theoretical calculations: a) the case where the critical (fiducial) density is $n_0 = 1.5 n_s$ and for $n \geq n_0$ the speed of sound is fixed to the value $v_s = c$ (EoS/maxstiff), b) the case where the fiducial density is $n_0 = 1.5 n_s$ and for $n \geq n_0$ the speed of sound is fixed to the value $v_s = c/\sqrt{3}$ (EoS/minstiff), and c) the case where the for $n \geq n_{c-crust}$ we simple employ the selected EoS without constraints (EoS/normal).

3 The Nuclear Models

In the present work we employed various relativistic and non-relativistic nuclear models, which are suitable to reproduce the bulk properties of nuclear matter at low densities, close to saturation density as well as the maximum observational neutron star mass (Refs. [4, 5]).

The momentum-dependent interaction model: The momentum-dependent interaction (MDI) model used here, was already presented and analyzed in previous papers [17, 18]. The MDI model is designed to reproduce the results of the microscopic calculations of both nuclear and neutron-rich matter at zero temperature and can be extended to finite temperature.

The momentum-dependent relativistic mean-field model: The relativistic formulation of the nuclear matter problem is based on the well-known quantum hadrodynamics (QHD) [19–22]. Here we adopt an RMF approach with non-linear derivative interactions, the so-called non-linear derivative (NLD) model (see Ref. [23, 24] for details). It is suitable for applications in systems beyond saturation density, because it contains explicitly the momentum dependence of the interaction.

The HLPS model: Recently, Hebeler *et al.* [25, 26] performed microscopic calculations based on chiral effective field theory interactions to constrain the properties of neutron-rich matter below nuclear densities. It explains the massive neutron stars of $M = 2M_{\odot}$.

The H-HJ model: Heiselberg and Hjorth-Jensen [27] adopted a simple form for the energy per particle in nuclear matter (hereafter H-HJ model). This model is suitable for applications in neutron stars studies.

The Skyrme models: Finally, we also perform calculations using the well-known Skyrme parametrization. The parametrization is given in Refs. [28, 29].

4 Tidal Polarizability

Gravitational waves from the final stages of inspiraling binary neutron stars are expected to be one of the most important sources for ground-based gravitational wave detectors [30–34]. Flanagan and Hinderer [30] have recently pointed out that tidal effects are also potentially measurable during the early part of the evolution when the waveform is relatively clean. The tidal fields induce quadrupole moments on the neutron stars. The response of the neutron star is described by the dimensionless so-called Love number k_2, which depends on the neutron star structure and consequently on the mass and the EoS of the nuclear matter. The tidal Love numbers k_2 is obtained from the ratio of the induced quadrupole moment Q_{ij} to the applied tidal field E_{ij}:

$$Q_{ij} = -k_2 \frac{2R^5}{3G} E_{ij} \equiv -\lambda E_{ij}, \tag{2}$$

where R is the neutron star radius and $\lambda = 2R^5 k_2/3G$ is the tidal polarizability. The tidal Love number k_2 depends on the compactness parameter $\beta = GM/Rc^2$ and the quantity y_R [30,31]. Actually, y_R is determined by solving the following differential equation for y

$$r\frac{dy(r)}{dr} + y^2(r) + y(r)F(r) + r^2Q(r) = 0,\ y(0) = 2,\ y_R \equiv y(R) \tag{3}$$

where $F(r)$ and $Q(r)$ are functionals of $\mathcal{E}(r)$, $P(r)$ and $M(r)$ [33]. Equation (3) must be integrated with the TOV equations using the boundary conditions $y(0) = 2$, $P(0) = P_c$ and $M(0) = 0$. The solution of the TOV equations provides the mass M and radius R of the neutron star, while the corresponding solution of the differential Eq. (3) provides the value of $y_R = y(R)$. In addition, the combined tidal effects of two neutron stars in a circular orbits are given by a weighted average of the quadrupole responses [30, 33],

$$\tilde{\lambda} = \frac{1}{26}\left[\frac{m_1 + 12m_2}{m_1}\lambda_1 + \frac{m_2 + 12m_1}{m_2}\lambda_2\right], \tag{4}$$

where $\lambda_1 = \lambda_1(m_1)$ and $\lambda_2 = \lambda_2(m_2)$ are the tidal deformabilities of the two neutron stars and $M = m_1 + m_2$ the total mass. The symmetric mass ratio is defined as $h = m_1 m_2 / M^2$. As pointed out in Ref. [33], the universality of the neutron star EoS allows one to predict the tidal phase contribution for a given binary system from each EoS. In this case the weighted average $\tilde{\lambda}$ is usually plotted as a function of chirp mass $\mathcal{M} = (m_1 m_2)^{3/5}/M^{1/5}$ for various values of the ratio h.

5 Results and Discussion

Figure 1(a) shows the radius-mass relation of neutron stars using various EoS without any restriction on the speed of sound (except the relativistic one). One can see, that all hadronic models can reproduce the recent observation of two-

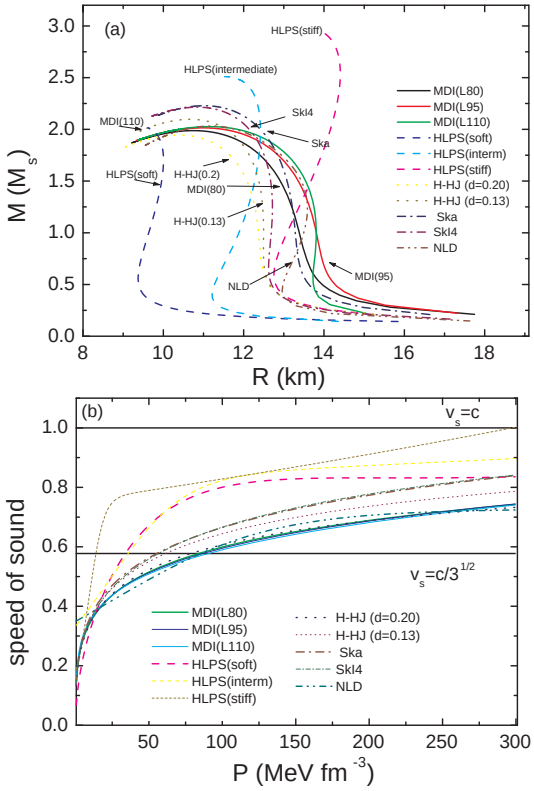

Figure 1. (a) Mass-radius diagram for the equations of state used in the present work. (b) The speed of sound dependence on the pressure for the EoSs used in the paper. The two specific upper bounds considered in the present work $v_s = c$ and $v_s = c/\sqrt{3}$ are also indicated.

solar massive neutron stars. In general, the stiffer EoS (at high densities) the higher the maximum neutron star mass. Before starting to analyze the effects of the speed of sound limits on the EoS, we show in Figure 1(b) the density dependence of this quantity for the various EoSs used here. It is obvious that almost all the EoSs are causal even for high values of the pressure (the only exception is the case HLPS (stiff) where the v_c exceed the c for relative low pressure). However, it is worth mentioning that in all hadronic models, used in the present study, the speed of sound v_s reaches the bound limit $c/\sqrt{3}$ at relative low values of the pressure (for $P \leq 100\ \mathrm{MeV} \cdot \mathrm{fm}^{-3}$). This feature has dramatic effect on the maximum mass configuration. This is now discussed in Figure 2(a). The neutron star configurations with the five selected EoSs in the normal case (no constraints on v_s except the conventional $v_s < c$) are also shown for comparison. It is seen that the upper bound limit of the speed of sound imposes

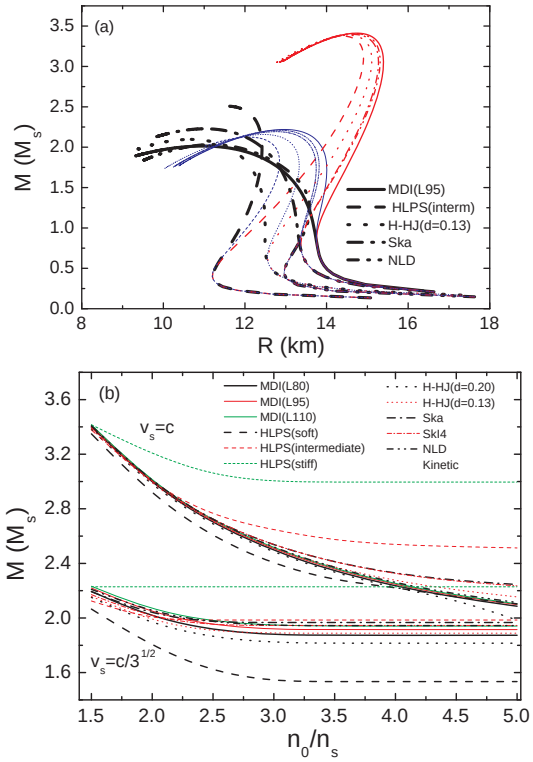

Figure 2. (a) The mass-radius diagram for five EoSs (EoS/normal case, line with thick width) in comparison with the corresponding maximum mass configuration results of the EoS/minstiff case (line with medium width) and and EoS/maxstiff case (line with thin width). (b) The maximum mass of neutron stars as a function of the critical density n_0 for the two upper bounds for the speed of sound $v_s = c$ and $v_s = c/\sqrt{3}$.

essential changes to the neutron star structure. The higher the limit after the fiducial density, the stiffer the corresponding EoS. This results to a higher value for the maximum neutron star mass. By setting the upper limit to $v_s = c/\sqrt{3}$ the stiffness of the EoS weakens at higher densities and consequently the neutron star mass reduces to lower values.

To further clarify the critical density dependence on $M_{\max}$, we display in Figure 2(b) the dependence of the maximum mass for the chosen EoS, on the fiducial density n_0. We considered two upper bounds for the speed of sound: $v_s = c$ and $v_s = c/\sqrt{3}$. First, one sees an overall reduction of the neutron star mass with increasing critical density. Using the density behavior of the $v_s = c/\sqrt{3}$ constraint in the calculations, the neutron star mass first decreases and then approaches a constant value, which is characteristic for each EoS. It is remarkable that in all cases the neutron star mass drops below the experimental value of two solar masses (the only exception is the stiff case of the HLPS model). Therefore, the assumption of $v_s = c/\sqrt{3}$ value as the upper limit for the speed of sound in compressed matter would exclude particular EOSs which contradict with recent astrophysical observation of massive neutron stars. Our results are similar to those of Bedaque and Steiner [12]. On the other hand, when the causality limit $v_s = c$ is imposed, the upper bound on the maximum mass significantly increases as is well known from previous studies and the relevant predictions (see Refs. [10, 11] and references therein). It is noted that recently an upper bound of neutron star masses was obtained from an analysis of short gamma-ray bursts [35]. Assuming that the rotation of the merger remnant is limited only by mass-shedding, then the maximum gravitational mass of a nonrotating neutron star is $M_{\max} = (2 - 2.2)\ M_{\odot}$ [35]. Furthermore, the authors of Ref. [36], using population studies, determined the distribution of these compact remnants to compare with the observations. All these recent analyses, although dealing with the problem of the upper bound of neutron star mass in different ways, predict as an absolute upper limit for the maximum neutron star masses $M_{\max} \geq 2M_{\odot}$. This prediction is in accordance with the recent observations [4, 5].

We propose now an additional approach to investigate the upper bound of v_s. It is well known that the influence of the star's internal structure on the waveform is characterized by the value of the tidal polarizability λ. It was found that λ is sensitive to the details of the equation of state. Furthermore, the tidal polarizability exhibits very strong dependence on the radius R and consequently on the details of the equation of state at low and high values of the baryons density. The critical density dependence on a few bulk neutron star properties is displayed in Figure 3. In particular, we display the critical density dependence on the radius R (Figure 3(a)), on the tidal polarizability λ (Figure 3(b)) and on the dimensional polarizability $\Lambda = \frac{3k_2}{2}\left(\frac{c^2 R}{GM}\right)^5$ (Figure 3(c)) for the two bounds of the speed of sound. Obviously, the effects are more pronounced for low values of n_0 and for high values of neutron star mass. All the mentioned quantities are basic ingre-

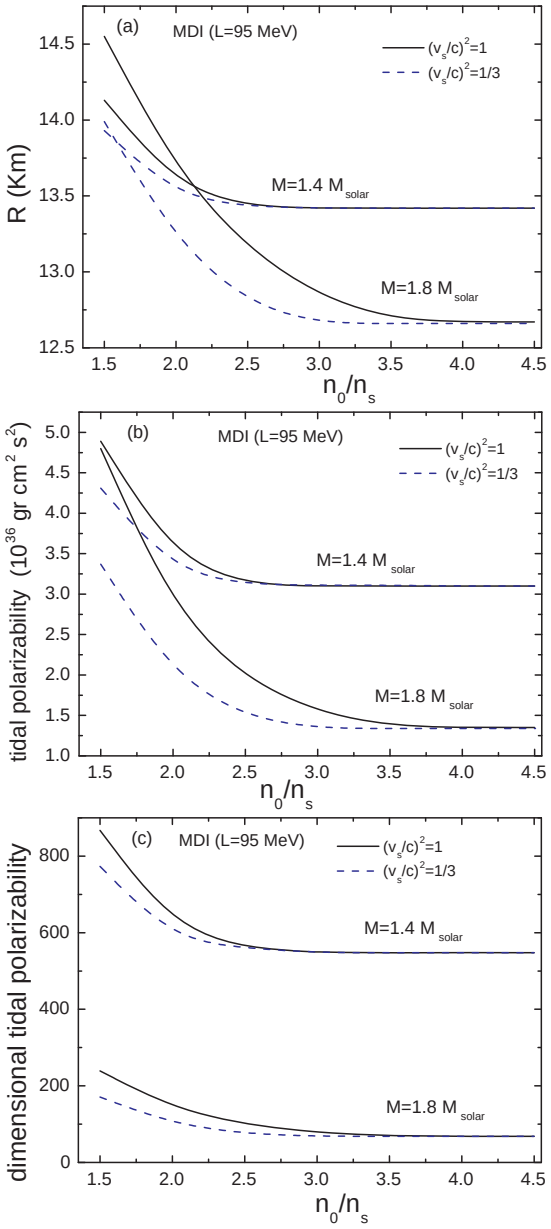

Figure 3. The critical density dependence on: (a) the radius R, (b) the tidal polarizability λ and (c) and on the dimensional polarizability Λ for the two bounds of the speed of sound and for two neutron stars masses.

dients of the difference of phase $\Delta\Phi$ of a gravitational wave, between a spinless black hole-black hole and black hole- neutron star binary system [37, 38]. Consequently, the measure of $\Delta\Phi$ will provides robust constraints on EoS.

The tidal polarizability is an important quantity, as it can be deduced from observations on neutron star binary systems. This is shown in Figure 4(a). The *signature* of the maximum mass configuration on the values of λ is obvious. In particular, we found that λ takes a wide range of values ($\lambda \sim (1-5) \times 10^{36}$ gr cm^2 s^2) for the employed EoS (EoS/normal case). Because λ is sensitive to the neutron star radius, this quantity is directly affected by the EoS. An EoS leading to large neutron star radii will also give high values for the tidal polarizability λ (and vice versa). The constraints of the upper bound on the speed of sound (EoS/minstiff) lead to a non-negligible increase of λ for high values of neutron star mass. However, in the EoS/maxstiff case the corresponding increase of λ is substantial, compared to the EoS/normal case. Moreover, in this case the values of λ remain measurable even for very high values of the mass. This behavior results from the strong dependence of λ on the radius R. Specifically, the increase of the upper bound on the speed of sound influences significantly the maximum mass configuration in two ways. First, a dramatic increase of the upper bound of $M_{\rm max}$. Second, the neutron star radius is significantly increased. A radius increase by 10% leads already to a rise of the tidal polarizability λ by 60%.

In the same figure, the ability to measure the tidal polarizability from the Advanced LIGO and the Einstein Telescope is indicated. The region of possible observations with the Advanced LIGO is indicated by the unshaded region. The Einstein Telescope has larger ability and will be able to measure the tidal polarizability in the unshaded and light shaded region (see also Ref. [33]).

Note that the Einstein Telescope will be able to measure λ even for neutron stars with a masses up to $2.5\ M_\odot$ and consequently to constrain the stifness of the equation of state. To be more precise, from these observations one will be able to test the upper bound $v_s = c/\sqrt{3}$. The simultaneous measurements of neutron star masses M and tidal polarizabilities λ will definitely help to better clarify the stiffness limits of the equation of state. These features are shown in our calculations. For instance, the model within the EoS/normal case predicts values of the tidal polarizability λ, which are out of the detection region of the Einstein Telescope (see also the studies in Refs. [33]). On the other hand, the calculations with the EoS/minstiff model lead to λ values, which are just near that sensitivity region. The EoS/maxstiff results show a clear observable signature. In particular, for intermediate mass neutron stars $(1-2M_\odot)$ with large values for the tidal polarizability λ the upper bound $v_s = c/\sqrt{3}$ seems to be violated. In view of the above analysis we conjecture that it is possible with the third-generations detectors to examine closely the extent of the stiffness of the neutron star EoS and the relative constraints on the upper bound on the speed of sound.

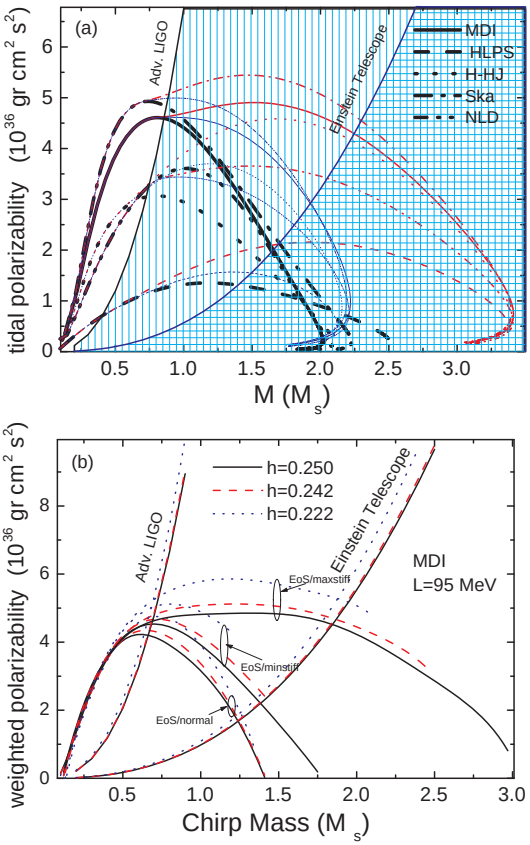

Figure 4. (a) The tidal polarizability λ of a single neutron star as a function of the mass for the five selected EoS's (EoS/normal case) in comparison with the corresponding maximum mass configurations results (EoS/minstiff and EoS/maxstiff cases). The notation is as in Figure 2(a). The ability detection region of the Advanced LIGO is the unshaded region and the corresponding of the Einstein Telescope by the unshaded and light shaded region (see text for more details and also Ref. [33]). (b) The weighted tidal polarizability $\tilde{\lambda}$ as a function of the chirp mass $\mathcal{M}$ for various values of the symmetric ratio η for the three considered cases which correspond to the MDI (L95) EoS. The uncertainty $\Delta\tilde{\lambda}$ in the $\tilde{\lambda}$ measure of the Advanced LIGO and the corresponding of the Einstein Telescope are also indicated (for more details see text and also Ref. [33]).

We now discuss the weighted tidal polarizability $\tilde{\lambda}$ as a function of the chirp mass $\mathcal{M}$ varying the symmetric ratio h, as shown in Figure 4(b). We consider again the main three cases (EoS/normal, EoS/minstiff, and EoS/max stiff) where for the intermediate region of the density we employ the MDI model with the slope parameter $L = 95$ MeV. The three values of the symmetric ratio (0.25, 0.242, 0.222) correspond to the mass ratio m_2/m_1 (1.0, 0.7, 0.5) (for more details see

also Ref. [33]). The uncertainty $\Delta\tilde{\lambda}$ in measuring $\tilde{\lambda}$ of the Advanced LIGO and the corresponding of the Einstein Telescope are also presented. From Figure 4(b) it is concluded that the upper bound of the speed of sound and consequently the maximum mass configuration affects appreciable the chirp mass-weighted tidal polarizability dependence. This effect is more pronounced for chirp masses $\mathcal{M} > 0.5\ M_{\odot}$. In particular, for high values of $\mathcal{M}$, the Einstein telescope has the sensibility to distinguish the mentioned dependence.

We believe that the simultaneous measure of M and λ will help to better understand the stiffness limit of the equation of state. In particular, observations with third-generation detectors, will definitely provide constraints for the stiffness of the EoS at high density. This is expected to provide more information related to the upper bound of the speed of sound in hadronic matter. The accurate estimate of the upper bound of the speed of sound in hadronic matter is greatly important for a consistent prediction of the maximum mass of a neutron star. The future detection and analysis of gravitational waves in binary neutron star systems is expected to shed light on this problem.

Acknowledgments

This work supported by the DAAD Germany-Greece grant ID 57340132 as well as the European Cooperation in Science and Technology (COST) Action CA16214.

References

[1] J.B. Hartle (1978) *Phys. Rep.* **46** 201.
[2] M. Coleman Miller, J.M. Miller (2015) *Phys. Rep*. **548** 1.
[3] B. Kiziltan, A. Kottas, M.De Yoreo, S.E. Thorsett (2013) *Astrophys. J.* **778** 66.
[4] P. Demorest, T. Pennucci, S. Ransom, M. Roberts, J. Hessels (2010) *Nature* **467** 1081.
[5] J. Antoniadis, P.C. Freire, N. Wex, T.M. Tauris, R.S. Lynch, *et al.* (2013) *Science* **340** 1233232.
[6] P. Haensel, A.Y. Potekhin, D.G. Yakovlev (2007) *Neutron Stars 1: Equation of State and Structure*, Springer-Verlag, New York.
[7] C.E. Rhoades, R. Ruffini (1974) *Phys. Rev. Lett.* **32** 324.
[8] V. Kalogera, G. Baym (1996) *Astrophys. J.* **470** L61.
[9] S. Koranda, N. Stergioulas, J.L. Friedman (1997) *Astrophys. J.* **488** 799.
[10] J.M. Lattimer, M. Prakash (2011) *in From Nuclei to Stars*, edited by S. Lee, World Scientific, Singapore, p. 275.
[11] N. Chamel, P. Haensel, J.L. Zdunik, A.F. Fantina (2013) *Int. J. Mod. Phys. E* **22** 1330018.
[12] P. Bedaque, A.W. Steiner (2015) *Phys. Rev. Lett.* **114** 031103.
[13] A.G. Sabbadini, J.B. Hartle (1973) *Astrophys. Space Sci.* **25** 117.

[14] L.D. Landau, E.M. Lifshitz (1987) *Fluid Mechanics*, Pergamonm Oxford, pp. 251-254.
[15] G. Baym, C. Pethik, P. Sutherland (1971) *Astrophys. J.* **170** 299.
[16] Ch.C. Moustakidis, T. Niksic, G.A. Lalazissis, D. Vretenar, P. Ring (2010) *Phys. Rev. C* **81** 065803.
[17] Madappa Prakash, I. Bombaci, Manju Prakash, P.J. Ellis, J.M. Lattimer, R. Knorren (1997) *Phys. Rep.* **280** 1.
[18] Ch.C. Moustakidis (2015) *Phys. Rev. C* **91** 035804.
[19] H.-P. Duerr (1956) *Phys. Rev.* **103** 469.
[20] J. Walecka (1974)*Annals Phys.* **83** 491.
[21] B.D. Serot, J.D. Walecka (1997) *Int. J. Mod. Phys. E* **6** 515.
[22] D. Vreternar, A.V. Afanasjev, G.A. Lalazissis, P. Ring (2005) *Phys. Rep.* **409** 101.
[23] T. Gaitanos, M.M. Kaskulov (2013) *Nucl. Phys. A* **899** 133.
[24] T. Gaitanos, M. Kaskulov (2015) *Nucl. Phys. A* **940** 181.
[25] K. Hebeler, J.M. Lattimer, C.J. Pethick, and A. Schwenk, Phys. Rev. Lett. **105**, 161102 (2010).
[26] K. Hebeler, J.M. Lattimer, C.J. Pethick, and A. Schwenk, Astrophys. J. **773**, 11 (2013).
[27] H. Heiselberg, M. Hjorth-Jensen (2000) *Phys. Rep.* **328** 237.
[28] E. Chabanat, P. Bonche, P. Haensel, J. Meyer, R. Schaeffer (1997) *Nucl. Phys. A* **627** 710.
[29] M. Farine, J.M. Pearson, F. Tondeur (1997) *Nucl. Phys. A* **615** 135.
[30] E.E. Flanagan, T. Hinderer (2008) *Phys. Rev. D* **77** 021502.
[31] T. Hinderer (2008) *Astrophys. J.* **677** 1216.
[32] T. Damour, A. Nagar (2009) *Phys. Rev. D* **80** 084035.
[33] T. Hinderer, B.D. Lackey, R.N. Lang, J.S. Read (2010) *Phys. Rev. D* **81** 1230161.
[34] B.D. Lackey, L. Wade (2015) *Phys. Rev. D* **91** 043002.
[35] S. Lawrence, J.G. Tervala, P.F. Bedaque, M.C. Miller (2015) *Astrophys. J.* **808** 186.
[36] C.L. Freyer, K. Belczynski, E.R. Ruiz, S. Rosswong, G. Shen, A.W. Steiner (2015) *Astrophys. J.* **812** 24.
[37] B.D. Lackey, K. Kyutoku, M. Shibata, P.R. Brady, J.L. Friedman (2014) *Phys. Rev. D* **89** 043009.
[38] E.D. Van Oeveren, J.L. Friedman (2017) *Phys. Rev. D* **95** 083014.